Astronomy & Astrophysics manuscript no. aa58610-25
February 6, 2026

Early growth of massive black holes in dynamical dark energy models with negative cosmological constant

N. Menci[1], M. Castellano[1], P. Mukherjee[2], D. Roberts[3], P. Santini[1], A.A. Sen[2], and F. Shankar[3]

[1] Istituto Nazionale di Astrofisica (INAF), Osservatorio Astronomico di Roma, Via Frascati 33, 00078 Monte Porzio Catone (RM), Italy
[2] Centre for Theoretical Physics, Jamia Millia Islamia, New Delhi-110025, India
[3] School of Physics & Astronomy, University of Southampton, Highfield, Southampton SO17 1BJ, UK

Preprint online version: February 6, 2026

ABSTRACT

Context. Recent results from combined cosmological probes indicate that the Dark Energy component of the Universe could be dynamical. The simplest explanation envisages the presence of a quintessence field rolling into a potential, where the Dark Energy energy density parameter $\Omega_{DE} = \Omega_\Lambda + \Omega_x$ results from the contribution of the ground state energy Ω_Λ and the scalar field energy Ω_x. Provided that $\Omega_{DE} \approx 0.7$, negative values of Ω_Λ can be consistent with current measurements from cosmological probes, and could help in explaining the large abundance of bright galaxies observed by JWST at $z > 10$, largely exceeding the pre-JWST expectations in a ΛCDM Universe.

Aims. Here we explore to what extent such a scenario can account also for the early presence of massive Black Holes (BHs) with masses $M_{BH} \gtrsim 10^7\ M_\odot$ observed at $z \gtrsim 8$, and for the large over-abundance of AGN with respect to pre-JWST expectations. Our aim is not to provide a detailed description of BH growth, but rather to compute the maximal BH growth that can occur in cosmological models with negative Ω_Λ under the simple assumption of Eddington-limited accretion onto initial light Black Hole seeds with mass $M_{seed} \sim 10^2\ M_\odot$ originated from PopIII stars.

Methods. To this aim we develop a simple analytic framework to connect the growth of dark matter halos to the maximal growth of BHs within the above assumptions.

Results. We show such models can account for present observations assuming values of $\Omega_\Lambda \approx -1$, simultaneously boosting both galaxy and AGN number counts without invoking any additional physics. This would allow us to trace the observed excess of bright and massive galaxies and the early formation of massive Black Holes and the abundance of AGN to the same cosmological origin.

Key words. Keywords should be given

1. Introduction

In recent years, major observational breakthroughs, largely provided by the James Webb Space Telescope (JWST), have severely challenged the canonical ΛCDM scenario for the formation of cosmic structures. These observations revealed a sensible excess of massive galaxies at $z \gtrsim 6$ (Labbé et al. 2023; Xiao et al. 2024; Casey et al. 2024) and of star forming, UV bright galaxies at $z \gtrsim 10$ (Castellano et al. 2022; Finkelstein et al. 2022; Atek et al. 2022; Whitler et al. 2022; Robertson et al. 2024; Finkelstein et al. 2023; Pérez-González et al. 2023; Donnan et al. 2022; Harikane et al. 2023; Bouwens et al. 2023; McLeod et al. 2023; Adams et al. 2024; Finkelstein et al. 2024; Pérez-González et al. 2025) over the pre-JWST models of galaxy formation in the ΛCDM scenario.

Such a fast growth of the galaxy stellar mass content of galaxies seems to be accompanied by an even faster growth of the mass M_{BH} of the Supermassive Black Holes (BHs) hosted in high redshift galaxies, which is thought to originate from the accretion of gas onto initial BH seeds, see Volonteri et al. (2021) for a review). BH masses as large as $M_{BH} \approx 10^{7-8.5}\ M_\odot$, as inferred from the broadening of Balmer lines, have now been found already at $z \sim 6 - 8.5$ (Kokorev et al. 2023; Harikane et al. 2023a; Maiolino, Roberto et al. 2024; Furtak et al. 2024; Juodžbalis et al. 2024), while at higher redshifts $z \gtrsim 10$ the observations of high-ionization lines (Maiolino, Roberto et al. 2024) and X-ray detections (Bogdán et al. 2024; Kovács et al. 2024) have led to infer BH masses as high as $M_{BH} = 10^{6.2-7.9}\ M_\odot$.

These high masses pose a crucial challenge for theoretical models of BH seeding and growth due to the lack of cosmic time available for their assembly, see reviews by Inayoshi & Ichikawa (2024); Fan et al. (2023). For instance, the assumption that the initial BH seeds are constituted by the remnants of metal-free PopIII with mass $M_{seed} \sim 10^2\ M_\odot$ (Carr & Rees 1984; Abel et al. 2002) and that the accretion is Eddington limited, seems to be excluded since in the ΛCDM framework there is not sufficient time to build up such high measured BH masses by $z \approx 8$, even assuming continuous accretion throughout the available cosmic time.

In addition to the large masses of high-redshift BHs, the demography of the BHs in accreting phase (the Active Galactic Nuclei, AGN) is also at variance with pre-JWST expectations (Harikane et al. 2023b; Maiolino et al. 2024a; Juodžbalis et al. 2025; Scholtz et al. 2025; Akins et al. 2024), with a number density of AGNs exceeding the pre-JWST measurements of the quasar abundance by more than one order of magnitude, at least at intermediate luminosities. Indeed, the AGN population revealed by JWST includes previously unseen, heavily reddened and extremely compact ($R_e \lesssim 100$ pc) objects at $4 \lesssim z \lesssim 10$, known as "little red dots" (Matthee et al. 2024; Furtak et al. 2023; Labbe et al. 2025; Kokorev et al. 2024; Greene et al. 2024;

Akins et al. 2024; Kocevski et al. 2025). Their compact size and peculiar spectra suggest that their emission is presumably dominated by obscured active galactic nuclei (AGN), an interpretation supported by the detection of broad emission lines in candidates possibly spectroscopically confirmed (and even by a direct measurement of the accreting BH mass, see Juodžbalis et al. (2025)), although alternative explanations exist Ananna et al. (2024) which suggest that their properties might be - at least partially - explained in terms of stellar emission Baggen et al. (2024).

Within the context of ΛCDM, all of the above observations call for the presence of different additional astrophysical processes that must be at work at high redshift $z \gtrsim 8$. While several approaches have been proposed to produce an accelerated early phase of star formation and UV emission with respect to the pre-JWST expectations - like stochastic star formation (Shen et al. 2023; Sun et al. 2023; Gelli et al. 2024), reduced dust attenuation (Ferrara, A. 2024), lower metallicity stellar populations or a top-heavy IMF (Trinca et al. 2024a; Yung et al. 2023), clumpy star formation (Somerville et al. 2025) and/or weaker supernova feedback (Dekel et al. 2023) - the presence of massive BH at high redshift $z \gtrsim 8$ and the large number density of AGN have been generally explained in terms of additional assumptions for the initial BH seeds and for the accretion properties of AGN. Theoretical models that have been employed to investigate the high-redshift growth of BHs (Trinca et al. 2024b; Porras-Valverde et al. 2025; LaChance et al. 2025; Cammelli et al. 2024; Dayal & Maiolino 2025; McClymont et al. 2026; Quadri et al. 2025) can simultaneously reproduce the over-massive nature and high space densities of the observed AGN by invoking episodic super-Eddington accretion (Madau et al. 2014; Volonteri et al. 2015), and/or assuming the existence of heavy seeds with masses $M_{seed} \sim 10^5\, M_\odot$ (Bromm & Loeb 2003; Begelman et al. 2006). Such seeds should form from the direct collapse of gas clouds in atomic-cooling halos with virial temperatures $T \sim 10^4$ K characterized by a pristine gas composition to avoid fragmentation and irradiated by a Lyman-Werner radiation intense enough to dissociate H_2 molecules so as to avoid star formation. Their formation thus requires rather peculiar conditions which are relatively rare, see, e.g., Schauer et al. (2017); Latif et al. (2022). As for the super-Eddington accretion, its plausibility and effectiveness within realistic conditions provided by the large-scale cosmological environment is subject to intense ongoing studies, see, e.g., Zhu et al. (2022); Ni et al. (2022); Bhowmick et al. (2022); Lupi et al. (2024)).

All the above conditions for star formation and BH growth at high redshift require substantial modification of the pre-JWST picture of galaxy formation of SMBH evolution at high redshift $z \sim 10$, while essentially preserving at lower redshifts the canonical picture of gradual gas conversion into stars and of BH growth through Eddington limited accretion, see, e.g.,Lai et al. (2024).

However, an alternative possibility is that the tension between the abundance and masses of high-redshift galaxies and BHs observed by JWST and the ΛCDM predictions originates in the assumed cosmological model. While the need for the introduction of substantial change or for more exotic physics affecting the early evolution of galaxies and BHs does not constitute on its own a conclusive evidence that the underlying cosmological model has to be revised, a growing body of independent observational evidence from cosmological probes suggests that the standard cosmological model, with dark energy (DE) described by a cosmological constant Λ, may be incomplete. In particular, the recent measurements (Adame et al. 2025; Lodha et al. 2025; Calderon et al. 2024; Abdul Karim et al. 2025; Andrade et al. 2025) of baryon acoustic oscillations (BAO) by the Dark Energy Spectroscopic Instrument (DESI), when complemented with Planck cosmic microwave background (CMB) data and type Ia supernovae (SNIa) distance moduli measurements (Scolnic et al. 2022; Brout et al. 2022; Rubin et al. 2025; Abbott et al. 2024; Sánchez et al. 2024; Vincenzi et al. 2024) yield evidence for a time-evolving, dynamical dark energy (DDE) (Adame et al. 2025; Abdul Karim et al. 2025; Lodha et al. 2025), with a confidence level ranging from $\sim 3\sigma$ to 4σ depending on the SNIa sample used in the constraints (Adame et al. 2025). The preference for DDE models compared to ΛCDM is robust with respect to the different parameterizations for the time evolution of DE (Lodha et al. 2025; Giarè et al. 2024).

The most straightforward interpretation of these results is that the DE is provided by the dynamics of a quantum field ϕ rolling over a potential $V(\phi)$, which would yield a time-changing equation-of-state parameter $w = [\dot\phi^2/2 - V(\phi)]/[\dot\phi^2/2 + V(\phi)]$ (Peebles & Ratra 1988; Ratra & Peebles 1988; Wetterich 1995; Caldwell et al. 1998). The vacuum state of such a field corresponds to a cosmological constant Λ, while the total DE density $\rho_{DE} = \rho_x + \rho_\Lambda$ is contributed by a dynamical part with energy density ρ_x and by the contribution of the ground state ρ_Λ. The observed low-redshift ($z \lesssim 1$) accelerated expansion of the Universe (Riess et al. 1998; Perlmutter et al. 1999) only requires the total DE density ρ_{DE} to be positive, leaving open the possibilities for positive and negative values of Λ. Although the commonly explored combinations of cosmic parameters generally assume positive ρ_Λ, corresponding to a de Sitter (dS) vacuum, the resulting scenarios have a number of drawbacks: e.g., constructing a stable, positive vacuum energy (a de Sitter vacuum) is notoriously difficult within string theory (Danielsson & Van Riet 2018; Vafa 2005; Palti 2019; Graña & Herráez 2021); in addition, when $\Omega_\Lambda > 0$ is assumed, the present cosmological constraints yield phantom-crossing behavior of the equation-of-state parameter w which evolves from values $w \leq -1$ at at $z \gtrsim 1$ to values $w \geq -1$ at later times, thus implying a phantom phase which would imply a negative kinetic contribution ϕ^2 to the equation of state parameter w (Ludwick 2017), and violate the null energy condition (Vikman 2005; Carroll et al. 2005; Nojiri et al. 2005; Oikonomou & Giannakoudi 2022; Trivedi 2024).

On the other hand, cosmological models characterized by a composite DE sector with a negative cosmological constant (NCC) $\Lambda < 0$ - corresponding to potentials $V(\phi)$ featuring a negative minimum, i.e., an anti-dS (AdS) vacuum - appear naturally within string theory, see Maldacena (1998); specific string-inspired models with a NCC are described in Murai & Takahashi (2025); Svrcek (2006); Luu et al. (2025). In fact, they have been proposed as attractive alternatives that can satisfy the late-time acceleration constraints still remaining consistent with the other standard cosmological observations (Cardenas et al. 2003; Poulin et al. 2018; Dutta et al. 2020; Visinelli et al. 2019; Ruchika et al. 2023; Di Valentino et al. 2021; Calderón et al. 2021; Sen et al. 2022; Malekjani et al. 2024; Adil et al. 2024; Mukherjee et al. 2025; Wang et al. 2025)). Indeed, recent studies by some of us have shown that such models can enhance high-redshift structure formation, making them promising candidates for explaining the JWST galaxy excess (Adil et al. 2023; Menci et al. 2024a,b; Chakraborty et al. 2025).

Motivated by such findings, here we explore the impact of assuming a DDE cosmology with a negative cosmological constant (NCC) on the early formation of massive BHs and on the demography of AGN. Specifically, we investigate whether NCC models can alone account for the recent JWST observa-

tions without introducing super-Eddington accretion phases or an initial population of heavy BH seeds, to assess whether such cosmological scenarios could constitute a viable, unified solution to all the issues raised by the high-z observations by JWST. Following the same line in our earlier works, we adopt a simple description to relate the stellar properties of galaxies to their DM halo, which is known to provide an excellent statistical description of the galaxy population at $z < 8$, while assuming initial BH seeds with mass $M_{seed} \approx 10^2\, M_\odot$ originating from PopIII stars, and Eddington limited accretion. Under such conditions, we then compute the maximal growth (corresponding to continuous accretion at the Eddington rate) of massive BHs assuming NCC cosmologies, and compute the corresponding maximal masses of high-redshift SMBHs and the impact on the AGN demography. The paper is organized as follows: In Sect. 2 we describe the NCC DE models and their impact on the Universe expansion and on the growth of cosmic structures. In Sect. 3 we recall how the abundance of DM halos is derived in such cosmological models, and how we relate the DM halo mass of the host galaxies to the SMBH masses and to the AGN accretion rate assuming continuous accretion at the Eddington limit and BH seeds with mass $10^2\, M_\odot$. Based on such a model, in Sect. 4 we compare the growth of BH masses and the AGN abundance at $z \gtrsim 5$ with recent JWST observations. Sect. 5 is devoted to discussion, while in Sect. 6 we present our conclusions.

2. Dark energy models

We consider a DE sector consisting of a cosmological constant $\Lambda \gtrless 0$ with associated vacum energy density $\rho_\Lambda = \Lambda/8\pi G$ which can be positive or negative, corresponding to a se Sitter (dS) or Anti-de Sitter (AdS) vacuum respectively. On top of this we consider a DE component with energy density $\rho_x(a) > 0$ which evolves with the expansion factor $a = 1/(1+z)$. Rather than focusing to a specific model for the evolving DE component, we parametrize the time evolution of its equation-of-state (EoS) parameter $w_x(a)$ using the widely adopted Chevallier-Polarski-Linder (CPL) form (Chevallier & Polarski 2001; Linder 2003):

$$w_x(z) = w_0 + w_a(1-a). \tag{1}$$

where w_0 describes the behavior of DE in the local Universe, the value of w_a describes its evolution back in cosmic time.

This parametrization captures the EoS behavior in several physical DE models as discussed in Linder (2003, 2006, 2008b,a); Scherrer (2015)) (see alsoPerkovic & Stefancic (2020) for a comparison among different parametrization proposed in the literature), and allows us to compare with earlier works.

The energy density of the evolving DE component then evolves according to the following:

$$\rho_x(a) = \Omega_x \rho_{c0} a^{-3(1+w_0+w_a)} e^{[-3w_a(1-a)]}. \tag{2}$$

where $\Omega_x \equiv \rho_x(1)/\rho_{c0}$ is the density parameter of the evolving DE component and ρ_{c0} is the critical density. Assuming a spatially flat Friedmann-Lemaître-Robertson-Walker Universe, the evolution of the Hubble rate (with respect to its present value H_0) in the matter-dominated era is governed by the following equation:

$$E^2(a) \equiv H^2(a)/H_0^2 = \Omega_m\, a^{-3} + \Omega_\Lambda + \Omega_x a^{-3(1+w_0+w_a)} e^{[-3w_a(1-a)]} \tag{3}$$

where Ω_m is the matter density parameter, $\Omega_\Lambda \equiv \Lambda/3$ is the density parameter associated with the cosmological constant, and $\Omega_m + \Omega_\Lambda + \Omega_x = 1$ holds. The density parameter of the combined DE sector is $\Omega_{DE} \equiv \Omega_x + \Omega_\Lambda$. Although Ω_Λ can be negative, the density parameter associated to the *total* DE density has to be $\Omega_{DE} \approx 0.7$ in order to be able to drive the observed cosmic acceleration at low redshift $z \lesssim 1$.

We notice that, in order to agree with observations, more negative values of Ω_Λ need to be compensated by more negative values of w_x, moving towards the phantom regime (Visinelli et al. 2019; Sen et al. 2022; Adil et al. 2023). These considerations lead to upper limits of order unity in $|\Omega_\Lambda|$, corresponding to a negative vacuum energy density $\lesssim 10^{-123}$ in Planck units. Although this may seem to represent the usual problem related to the small absolute value of the cosmological constant, recent studies (Demirtas et al. 2021, 2022) have shown that supersymmetric AdS_4 vacua of the above magnitude naturally arise in the framework of string theory.

3. Method

We build a flexible and transparent analytic model that can provide upper limits to the growth of galaxies and their central supermassive BHs associated to DM structure formation in a dynamical dark energy framework. The steps we follow in our procedure are the following:

- We first generate a sample of host halo masses extracted from the halo mass function at an initial redshift $z_i = 20$.
- We then grow each central DM halo above 3.5σ of the primordial density field along its main progenitor branch using analytical recipes
- Within each DM halo we grow a BH via mergers and accretion. An upper limit on the growth of BHs due to mergers is obtained assuming that the fractional increase via mergers is directly linked to the fractional growth in host DM mass, while the growth via accretion is assumed to be a continuous process at the Eddington limit.
- From our mock sample of central DM haloes and their BHs we build the mean BH mass-halo mass relation which we then use to convert the halo mass function into a BH mass function.
- From the BH mass function we then derive the AGN luminosity function, a straightforward step as in our approach all BHs are continuously accreting (duty cycle equal to unity) at the Eddington limit.
- For completeness, in what follows we will also compute from our models the implied galaxy UV luminosity function at $z \gtrsim 10$.

The last step allows us to make a direct comparison with current data on the $z \sim 5-6$ AGN luminosity function, although the most revealing comparisons will be the ones at $z \gtrsim 7$. We note that in principle it would be more straightforward to carry out a direct comparison with the BH mass function, but current estimates are mostly available at $z < 6$, a time when the effects of a dynamical dark energy wear off. We also stress that for the conversion from halo to BH mass function we do not include any scatter as we are already assuming a strictly *maximal* growth for each BH, given that in our modelling even the tiniest growth in the DM host halo induces a parallel growth in the central BH, and the latter further grows via constant Eddington-limited accretion. We remind that we are not including any super-Eddington accretion as our aim is to understand whether a strictly Eddington-limited accretion starting from PopIII BH seeds could be a viable model in matching the newest high-z AGN data in the context of NCC cosmologies.

3.1. Abundance of collapsed objects

The abundance of collapsed objects in the Universe is described by the mass function $dN(M)/dM$. We briefly recall its computation in NCC cosmologies, computed for different values of Ω_Λ following the lines in Menci et al. (2022).

We base on the Press & Schechter approach (Peacock 1999; Padmanabhan 2002; Dodelson 2003) that relates the mass distribution to the properties of the linear perturbation density field. These are enclosed in the the variance $\sigma(M, a)$ of matter density fluctuations smoothed on the comoving scale corresponding to the mass scale M. In terms of the linear power spectrum of matter density fluctuations $P_L(k, a)$ computed at cosmic expansion factor a, the variance writes

$$\sigma^2(M, a) = \frac{1}{2\pi^2} \int_0^\infty dk\, k^2 P_L(k, a) W^2(k, R) \tag{4}$$

where $W(k, R) = 3[\sin(kR) - kR\cos(kR)]/(kR)^3$ is the Fourier transform of the real-space spherical top-hat window function of radius $R = (3M/4\pi\bar{\rho})^{1/3}$, and $\bar{\rho}$ is the mean comoving background matter density. The linear power spectrum $P_L(k, z)$ of matter density fluctuations as a function of wavenumber k at a given expansion factor a can further be expressed as:

$$P_L(k, z) = P_0 k^{n_s} T^2(k) D^2(a) \tag{5}$$

where P_0 is a normalization constant, which is fixed using the present-day mass variance (σ_8) on a scale of 8 $h^{-1}Mpc$, $T(k)$ is the CDM matter transfer function, and $D(a)$ is the linear growth factor normalized to 1 at present cosmic time. Assuming that halos form when the linear perturbations reach critical linear overdensity δ_c for collapse, the mass function takes the general form

$$\frac{dN}{dM} = \frac{\bar{\rho}}{M^2} \frac{d\ln\nu}{d\ lnM} \nu\, f(\nu) \tag{6}$$

where $\nu = \delta_c/\sigma(M, a)$ is the critical height of density perturbations relative to the r.m.s. value of the perturbations. In the following we adopt the Sheth and Tormen (Sheth & Tormen 1999) mass function

$$\nu\, f(\nu) = A\left(\frac{1}{\bar{\nu}^{2q}} + 1\right) \frac{\bar{\nu}^2}{\pi} e^{-\bar{\nu}^2/2} \tag{7}$$

where the parameters $A = 0.32$, $a = 0.71$ and $q = 0.3$ are related to the physics of collapse.

The growth factor $D(a)$ plays a major role in determining the extension to large masses of the mass distribution. The faster is the growth of density perturbations, the larger is the probability that rare, high-mass overdensities reach the threshold for collapse. The evolution of the growth factor is governed by the following equation (see, e.g., Adil et al. (2023) and references therein).

$$\delta'' + \left[\frac{3}{a} + \frac{E'(a)}{E(a)}\right]\delta' - \frac{3}{2}\frac{\Omega_m}{a^5 E^2(a)}\delta = 0\,, \tag{8}$$

where $'$ indicates a derivative with respect to the scale factor a, and $E(a) \equiv H(a)/H_0$ denotes the normalized expansion rate in 3. The equation shows how the growth of perturbations through gravitational instability is counter-acted by Hubble friction term due to the expansion of the Universe. For each chosen set of cosmological parameters determining the expansion rate 3 we numerically solve eq. 8.

Inspection of eq. 3 and 8 immediately shows the effect of introducing a negative Λ. At early times $a \to 0$ the term related to matter density $\Omega_m\, a^{-3}$ dominates over all other terms, so that $H(a)$ (and hence $D(a)$) is almost independent on the other cosmological parameters. Analogously, in the late time regime $a \to 1$ the expansion rate in 8 - and hence the growth factor $D(a)$ - reduces exactly to the ΛCDM case since $\Omega_x + \Omega_\Lambda = 1 - \Omega_m \approx 0.7$, and again assuming a NCC has no effect on the growth of perturbations.

However, at intermediate redshifts $z \sim 10 - 20$, the value of Ω_Λ appreciably affects $H(a)$; eq. 3 shows that for decreasing values of Ω_Λ (and particularly for negative values) a slower expansion rate $H(a)$ is obtained, resulting into larger growth factors in eq. 8. Thus, at such redshifts, we expect a larger abundance of massive objects compared to ΛCDM, as shown in fig. 1 in Menci et al. (2024b).

Extending the above Press & Schechter approach to derive the whole growth history of the DM halos through subsequent merging of DM condensations (see, e.g., Lacey & Cole (1993), it is possible to derive the mass growth of the main branch in a DM growth history due to accretion and merging of haloes. This reads (Neistein et al. (2006), see, also Liu et al. (2024); Correa et al. (2015))

$$\frac{1}{M(a)}\frac{dM}{dt} = -\sqrt{\frac{2}{\pi}}\frac{1}{\sqrt{\sigma^2(M/q) - \sigma^2(M)}}\frac{d[\delta_c/D(t)]}{da} \tag{9}$$

where q can be computed to be in the range $q = [2.1-2.3]$ for flat cosmologies, with an uncertainty which is an intrinsic property of the extended Press & Schecter theory. The comparison with up-to-date N-body simulations (Liu et al. 2024) showed that the above predictions match the simulations results with typical values for the residuals $\lesssim 0.2$. The authors in Correa et al. (2015) showed that in the high-redshift regime we are interested in this paper, the above rate can be written as

$$\frac{1}{M}\frac{dM}{dt} = A\, f(M_0)\, E(a) \tag{10}$$

leading to an exponential growth of the halo mass (as already obtained by Wechsler et al. (2002)). When the mass M is expressed in units $10^{12}\, M_\odot$ the normalization takes the value $A = 10^2\, h\, yr^{-1}$, and $f(M_0) = 1/\sqrt{\sigma^2(M_0/q) - \sigma^2(M_0)}$ depends on the final mass M_0 of the parent halo at $z = 0$. We have verified that our mass growth histories (computed with small time steps according to the prescriptions in Neistein et al. (2006)) agree with those obtained in the above mentioned papers.

3.2. The growth of black holes and stars in the host dark matter halos

To compute the growth of the BHs and stellar mass hosted in the evolving DM halos we adopt a simplified approach: the aim is not to achieve detailed and precise predictions for the abundance of supermassive BHs, but rather to derive the maximal BH growth that can be achieved in different NCC cosmologies under the most conservative assumptions for the physics of BH accretion and star formation.

To this aim, we first consider a grid of halo masses M at the initial redshift $z_i = 20$, for which we compute the growth of the halos according to eq. 9. This allows us to represent the average mass growth of each mass bin. Following an approach widely used in the literature (see, e.g., Volonteri et al.

(2003); Barausse (2012); Dayal et al. (2019)) we populate all halos collapsing from the large $\gtrsim 3.5\sigma$ peaks of the primordial density field (Madau & Rees 2001; Volonteri et al. 2003); in the ΛCDM case, this corresponds to populate halos with mass $M \geq 1.1\, h^{-1}\, 10^7\, M_\odot\, [(1+z)/20]^{-3/2}$ (Volonteri et al. 2003).

Since we are interested in computing the maximal BH mass growth in the light-seeds scenario, we start from BH seeds with mass $M_{seed} = 10^2\, M_\odot$. From such an initial mass, BHs can grow both by accretion and merging. Since our aim is to derive the maximal SMBH growth that can be achieved in different NCC cosmologies, we assume continuous accretion at the Eddington limit

$$M'_{ed}(a) \equiv \left(\frac{dM_{BH}}{da}\right)_{Edd} = \frac{1}{\dot{a}}\,\frac{4\pi G\, M_{BH}(t) m_p}{\sigma_T \epsilon_r c} \qquad (11)$$

where G is the gravitational constant, m_p is the proton mass, σ_T is the Thomson scattering optical depth, ϵ_r is the BH radiative efficiency and c is the speed of light. The BH mass accreted in the timestep Δa (in terms of the expansion factor a) as $M_{BH}(a + \Delta a) = M_{BH}(a) + (1-\epsilon_r) M'_{ed}(a) \cdot \Delta a$, where we assume a fiducial value $\epsilon_r = 0.1$ for the radiative efficiency of accreting BHs. This allows us to compute the BH mass in each DM halo at the next time step.

In the spirit of maximizing the BH growth in a given cosmological scenario, we assume an instantaneous merging scenario. We assume that BH masses merge following the same relative rate of their host halos given by eq. 9, i.e., that BH merging promptly follows that of their host halos. After updating the BH masses hosted in each DM halo after the above assumption, we iterate the procedure to get the average BH mass M_{BH} hosted in halos with DM mass M at a cosmic epoch t, up to a final time corresponding to $z_f = 4$. This procedure is strictly valid for the main branch of the merging histories of DM halos. However, here we focus on the high redshift evolution of DM halos (and SMBHs hosted therein), when, due to the extremely rapid merging events, the mass growth of halos can be described on average by the continuous mass accretion onto a main branch in eq. 9.

As for the average star formation rate associated to DM halos, we adopt a phenomenological representation of our knowledge about galaxy formation before the JWST era, thus assuming that the same physical processes that shape the baryon conversion into stars at $z \lesssim 10$ are also driving star formation at higher redshifts. Following the approach in Menci et al. (2024b), the DM mass M is related to the star formation rate of galaxies by $\dot{m}_* = \epsilon(M)\, f_b\, M$, where f_b is the cosmic baryon fraction. The efficiency $\epsilon(M)$ for the conversion of baryons into stars is taken from Mason et al. (2015) (see their fig. 1). This is a redshift-independent relation characterized by a maximal efficiency at masses $M \approx 10^{12}\, M_\odot$, and constitutes a phenomenological representation of our knowledge about galaxy formation before the JWST era. The star formation rate is related to the UV luminosity L through the relation $\dot{m}_*/\mathrm{M}_\odot\,\mathrm{yr}^{-1} = k_{UV}\, L/\,\mathrm{erg\,s^{-1}\,Hz^{-1}}$ with $k_{UV} = 0.7\, 10^{-28}$ assuming a Chabrier initial mass function (Madau et al. 2014), so that $L \propto \epsilon(M)\, M$. From the star formation rate above, the stellar mass m_* associated to a DM halo M can be computed analytically. Instead of performing time integration of $\dot{m}_*$ over the progenitors, we adopt a simple phenomenological approach proposed by Behroozi & Silk (2015) based on observed average relations. Measurements of the M_*-M relation at $z = 4 - 10$ show that their relation can be approximated as a power law $M_* = M_{*0}\,(M/M_0)^\alpha$ for DM masses $M \leq 5 \times 10^{11}\, M_\odot$ considered here, see Behroozi & Silk (2015); Behroozi et al. (2019, 2020). As noted by Behroozi & Silk (2015), this implies that the stellar and DM specific accretion rates are related by $\dot{M}_*/M = \alpha\, \dot{M}/M$. The stellar mass M_* can then be computed from $\dot{M}_*$ and from the DM specific accretion rate in eq. 9 from the observed values of α, which are within the range $\alpha = [1 - 1.5]$ (Behroozi & Silk 2015; Behroozi et al. 2019, 2020)). The uncertainties in M_* associated to the above range of values for α is considered when we derive the stellar mass M_*.

In the following, all distributions $dN(X,z)/dX = \left[dN(M,z)/dM\right](dM/dX)$ of any of the above observables X (i.e., the UV luminosity of galaxies, their star formation rate, stellar mass, BH mass and AGN luminosity) will be derived from the DM halo mass function 6 after connecting the halo mass M to the observable X following the modeling described above.

3.3. The cosmological framework

In our previous papers (Menci et al. 2024a,b) we have shown that quintessence models (with $w_0 \geq -1$ and $w_a \geq 0$) with negative Ω_Λ can provide a solution to the excess of both massive galaxies at $z \gtrsim 6$ and of luminous galaxies at $z \gtrsim 10$ observed by JWST. This is due to the accelerated growth of cosmic structures, as seen in fig. 1 in Menci et al. (2024b). In addition, such models do not yield crossing of the phantom regime, so that w remains in the non-phantom regime $w \geq -1$ throughout the cosmic history.

Since our aim here is to show that such cosmologies can provide a simultaneous solution to both the above excess and to the early growth of supermassive BHs at high redshifts (without invoking heavy seeds or Super-Eddington accretion), in the following we shall focus on such combinations. We further restrict the parameter space by requiring their consistency with the existing cosmological constraints. To this aim, we consider the following datasets:

i) latest data release from the Atacama Cosmology Telescope ACT DR6 (Louis et al. 2025) with a $Planck_{cut}$ likelihood from Planck PR3 data release Aghanim et al. (2020) (for details of the data combination, see Mukherjee et al. (2025) and references therein).

ii) the DESI-BAO DR2 (Abdul Karim et al. 2025) measurements for the redshift range $0.1 < z < 4.2$.

iii) the DES-SN5YR (Abbott et al. 2024; Sánchez et al. 2024) sample for SNIa luminosity measurements in the redshift range $0.1 < z < 1.13$ complemented by low-z SNIa measurements in the redshift range $0.025 < z < 0.1$.

We do not consider constraints from reionization. Although recent works in the literature (Chakraborty et al. 2025) have shown that the measurements of the cosmic reionization history may significantly s restrict the parameter space of DDE with negative cosmological constant, strongly limiting their boost to structure formation, the modeling of reionization is still affected by appreciable uncertainties. For instance, in the above paper, only the contribution of galaxy UV emission is considered as a source of reionization while, especially in view of our results below, a significant fraction of UV ionizing flux can result from AGN emission.

We run Markov Chain Monte Carlo (MCMC) methods to derive constraints on our set of cosmological parameters (for a full discussion of the methodology and the resulting constraints, we refer the reader to Mukherjee et al. (2025).

In Fig. 1, we show the allowed region in the $w_0 - w_a$ plane for the data combination mentioned above. As one can see, there is small but finite region in the parameter space which is always non-phantom, and where Ω_Λ is negative.

We explore the properties of such a region in a closer detail in Fig. 2, where we focus on non-phantom combinations (w_0, w_a) that match (within 2σ) the cosmological observations above. In the top-left panel, we show the average values of Ω_Λ corresponding to such (w_0, w_a) combinations. In the upper-right panel of Fig. 2 we show the values of σ_8 and of Ω_m, with the average value of Ω_Λ associated the non-phantom region of the w_0, w_a plane. For the same region, the whole distribution of Ω_Λ values resulting from our Monte Carlo procedure is shown in the bottom-left.

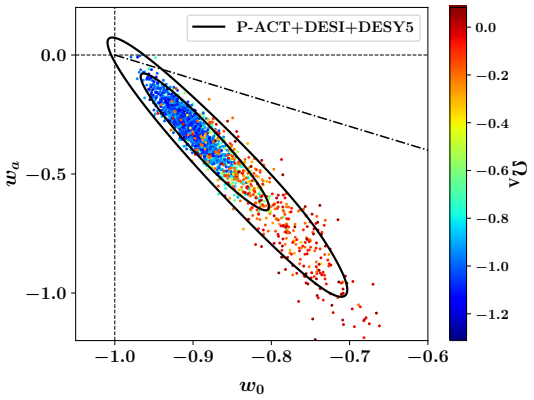

Fig. 1. 2D confidence contour in the $w_0 - w_a$ plane for our model using CMB+DESI+DES data combination. The Dash-Dotted line is phantom line. Above this line, the allowed region is always non-phantom, where as below this line, the allowed region is early phantom and late non-phantom. Dots represents different Monte Carlo realizations. The color code shows the value of Ω_Λ that allows for consistency with the above cosmological probes

Based on the results above, we shall consider here a fiducial choice $w_0 = -0.98$ $w_a = 0.08$ for the equation-of-state parameter, allowing Ω_Λ to assume all values in the distribution shown in the bottom-left panel of fig. 2. This ensures that the model considered here can be made consistent with the observed abundance of massive galaxies at $z \gtrsim 6$ (see Menci et al. (2024a)) and with the observed luminosity function of bright galaxies measured by JWST at $z \gtrsim 10$ that we show in Fig. 3. We have checked that our results do not differ appreciably when other combinations (w_0,w_a) are considered among the values defining the non-phantom regime ($w_0 \geq -1$ - $w_a \geq 0$) for the equation-of-state parameter represented in the upper right quadrant of Fig. 2. Inspection of Fig. 3 shows that values of $\Omega_\Lambda \approx -1$ can yield an abundance of high-redshift bright galaxies close to the observed values.

4. Results

Based on the above framework, we proceed to compute the growth of supermassive BHs in the framework of NCC cosmologies. As discussed in Sect. 3.2, our aim is not to achieve detailed and precise predictions for the abundance of BHs, but rather to derive the maximal BH growth that can be achieved in different NCC cosmologies under the most conservative assumptions for the physics of BH accretion and star formation. Following the above discussion, we populate all halos collapsing from the large $\gtrsim 3.5\sigma$ peaks of the primordial density with initial BH seeds with mass $M_{seed} \approx 10^2\, M_\odot$, and follow their evolution as described in Sect. 3.2 assuming continuous Eddington-limited accretion. Under the assumptions above, the maximal growth of

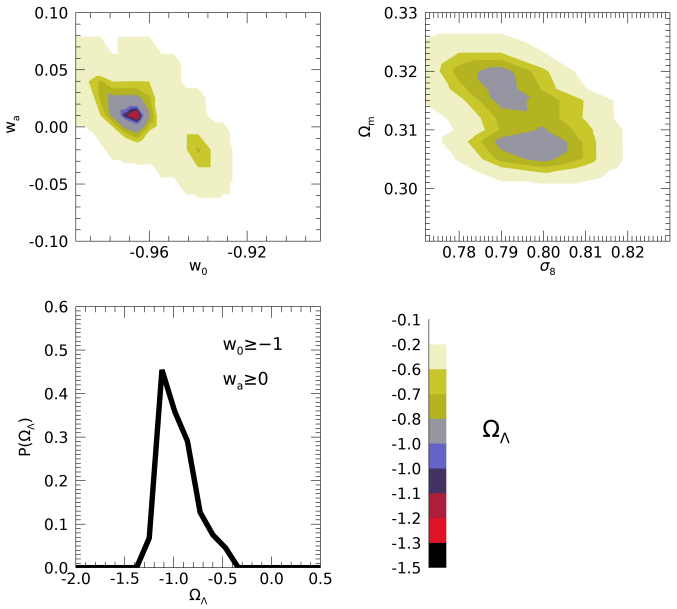

Fig. 2. Top-Left Panel: Based on our Monte Carlo procedure for the selection of (w_0-w_a, Ω_Λ) combinations combinations consistent (at 2-σ level) with the considered cosmological probes, we show as colored contours the average Ω_Λ as a function of (w_0-w_a). The color code is shown by the bar in the bottom-right of the figure.
Top-Right Panel: for the combinations ($w_0 \geq -1$, $w_a \geq 0$) considered here, we show the values of Ω_m and σ_8 consistent (at 2-σ level) with the considered cosmological probes. The color code refers to the average values of Ω_Λ corresponding to each combination, as shown by the bottom bar.
Bottom-Left Panel: the probability distribution of Ω_Λ resulting from our Monte Carlo procedure for the combinations ($w_0 \geq -1$, $w_a \geq 0$) considered here.

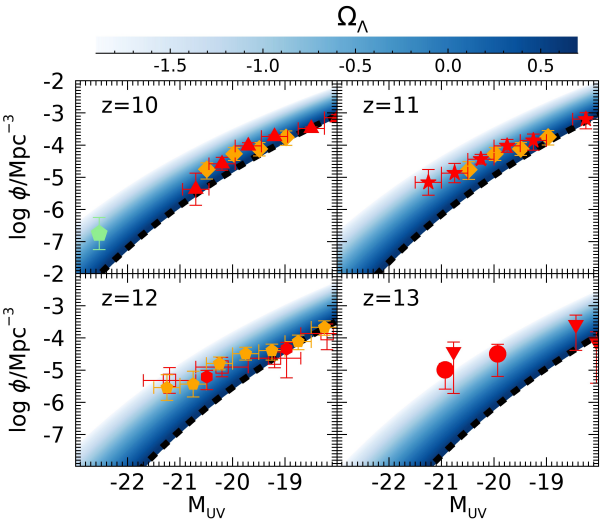

Fig. 3. The high redshift UV luminosity functions of galaxies for our fiducial combination of (w_0, w_a) in the different redshift bins shown in the labels. The color code corresponds the different values of Ω_Λ as shown in the top bar, while the dashed line mark the results for the standard ΛCDM cosmology. We compare with measurements from Finkelstein et al. (2023) (diamonds) Donnan et al. (2023) (stars) McLeod et al. (2023) (upward triangle) Harikane et al. (2023) (open square) Adams et al. (2024) (pentagon) Bouwens et al. (2022) (circle) Robertson et al. (2024) (downward triangle).

BHs hosted in halos corresponding to 3.5-peaks of the density

field is shown in Fig. 4 for our fiducial cosmological framework for different values of Ω_Λ.

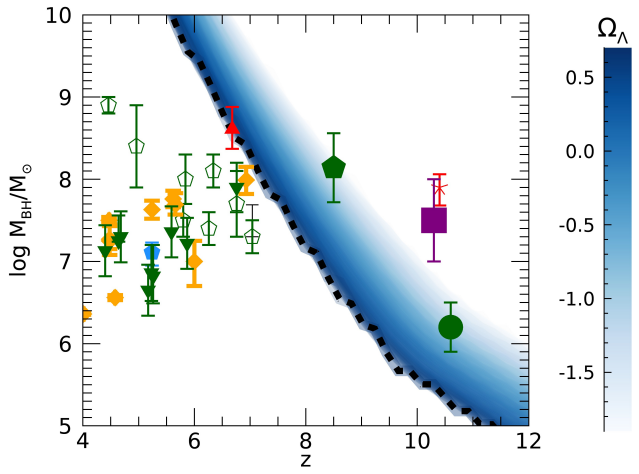

Fig. 4. The maximal growth of BHs from $M_{seed} = 10^2\ M_\odot$ at $z_{seed} = 25$ is shown for the different values of Ω_Λ shown in the color bar for our fiducial combination $w_0 = -0.98$, $w_a = 0.08$; the dashed line mark the result for the standard ΛCDM cosmology. To maximize the BH mass we assume continue Eddington-limited accretion. We compare these models to black holes measured by Bogdán et al. (2024) (solid square) Furtak et al. (2024) (cross) Greene et al. (2024) (empty petagons) Juodžbalis et al. (2024) (upward triangle) Harikane et al. (2023) (filled diamonds) Maiolino, Roberto et al. (2024) (downward triangles) Maiolino et al. (2024b) (solid circle) Kocevski et al. (2023) (solid pentagon)

As obtained in previous works in the literature (see, e.g., Dayal (2024) and references therein), in the ΛCDM cosmology with light BH seeds $M_\odot = 10^2\ M_\odot$, only BHs with mass $M_{BH} \lesssim 10^5\ M_\odot$ can be in place by $z \approx 10$, and $M_{BH} \lesssim 10^8\ M_\odot$ by $z \approx 8$, even under the assumption of continuous Eddington accretion.

On the other hand, assuming NCC cosmologies yields an accelerated growth of BHs at $z \geq 10$ (see 8) so as to allow for the presence of BHs as massive as $M_{BH} \sim 10^7\ M_\odot$ at $z \sim 10$ for $\Omega_\Lambda \approx -1$ without the need for Super-Eddington accretion or for heavy BH seeds. This shows that NCC cosmology can constitute an alternative solution to the problem posed by the presence of massive BHs at early cosmic epochs.

Motivated by such results, we proceeded to investigate whether the same cosmology can account for the other problem posed by the recent JWST observations, namely, the large number density of AGNs identified by JWST, both as type- I/type-II AGNs (see e.g. Harikane et al. (2023b); Maiolino, Roberto et al. (2024); Scholtz et al. (2025)) and as LRDs (see e.g. Matthee et al. (2024); Greene et al. (2024); Kokorev et al. (2024); Akins et al. (2024)). These studies show that the number density of JWST-detected systems lies between 1 and 2 dex larger than the extrapolation of the UV quasar luminosity function at $z \gtrsim 6$ (Shen et al. 2020) and higher than the estimated density from deep X-ray observations (Giallongo et al. 2015, 2019). Such large number densities exceed by ~ 1 order of magnitude the predictions of ΛCDM models implementing Eddington-limited models for the BH accretion (see Trinca et al. (2024b) and references therein).

Figure 5 shows the AGN bolometric luminosity function computed in different NCC models at $z = 5-7$ and $z = 7-9$. Again, our aim is not to test a detailed description of AGN accretion, but rather to show the maximal abundance of AGN that can be achieved in any given cosmological model under the assumption of Eddington-limited accretion and BH seeds with mass $10^2\ M_\odot$. The model results are compared with the recent estimates by Akins et al. (2024) based on JWST observations; the pre-JWST measurements by Shen et al. (2020) are also shown for comparison.

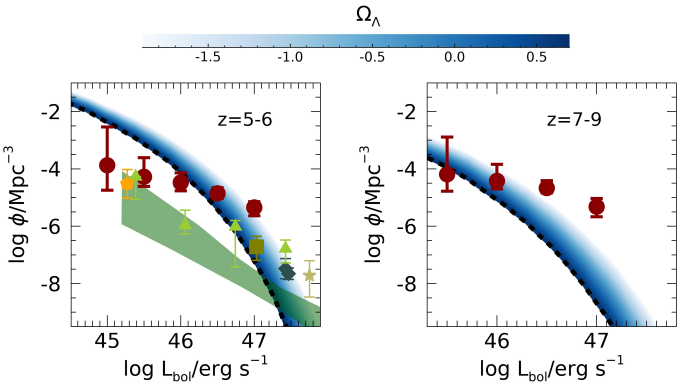

Fig. 5. The bolometric luminosity function of AGN under the assumption of continuous accretion at the Eddington rate is shown for the different values of Ω_Λ shown in the color bar for our fiducial combination $w_0 = -0.98$, $w_a = 0.08$; the dashed line mark the result for the standard ΛCDM cosmology. We compare with the measurements by Akins et al. (2024) based on JWST observations (red circles), derived under the assumption that the emission of LRD is entirely contributed by AGN, and by Harikane et al. (2023) (orange pentagon). For comparison, we also show the pre-JWST measurements by Shen et al. (2020) as a shaded area, by Glikman et al. (2011) (square), Grazian et al. (2023) (diamonds), and the X-ray measurement through Chandra COSMOS data by Barlow-Hall & Aird (2025) (triangles) and Barlow-Hall et al. (2023) (star).

As obtained in previous works in the literature (see, e.g. Trinca et al. (2024b)), in the Eddington-limited accretion scenario the predicted bolometric luminosity functions predicted in the ΛCDM cosmology drops by more than two orders of magnitude below the number density estimated by Akins et al. (2024) at the bright-end of the distribution. Also in this case, NCC models alleviated the discrepancy between observations and predictions, although the brightest point at $z \geq 7$ is still under-predicted.

However, the observational bolometric LF (Akins et al. 2024) reported here relies on the assumption that LRD emission is dominated by AGN. In fact, several studies suggest that both the stellar and the AGN components contribute to the SED (see e.g. Volonteri et al. (2024); Taylor et al. (2024)) thus resulting in a lower estimated AGN luminosity. Although this could bring the observed AGN luminosity function in better agreement with models (including those within the ΛCDM framework), this would result in a further additional component contributing to the stellar mass function and hence appreciably worsen the problems of current galaxy formation models in matching the abundance of massive galaxies at high redshifts $z \gtrsim 6$.

This is illustrated in fig. 6 where we compare the stellar mass function of galaxies in different cosmologies with the JWST measurements by Weibel et al. (2024). We show the increase in the abundance of massive galaxies that would be obtained if the emission of all LRD in the sample by Akins et al. (2024) was contributed by stars. In this extreme case a strong excess relative to the ΛCDM predictions would exist at $z \approx 7$, while a much better agreement would be obtained for NCC models. Although

such an excess is still to be confirmed by extending the portion of the sample which include MIRI measurements, this indicates that the tension with the ΛCDM predictions yield by the abundance of LRD would show up either in the luminosity function of AGN (at least under the assumption of Eddington-limited accretion) or in the stellar mass function. Future measurements, able to increase the accuracy of stellar mass measurement, will help to assess the issue.

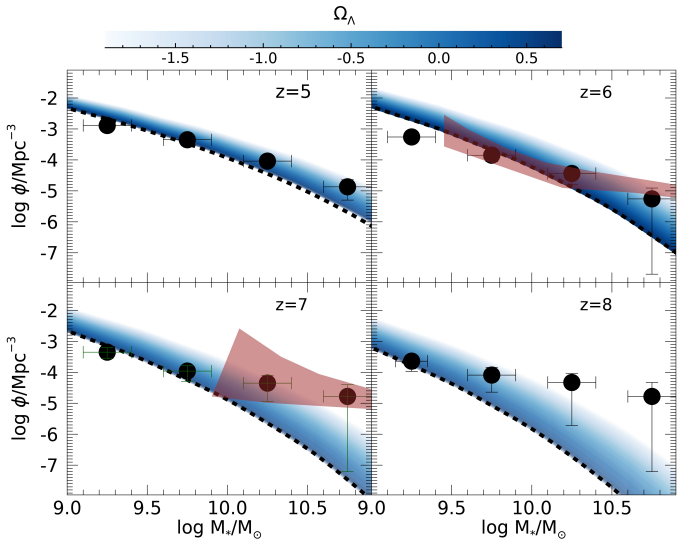

Fig. 6. The stellar mass function of galaxies for the different values of Ω_Λ shown in the color bar for our fiducial combination $w_0 = -0.98$, $w_a = 0.08$; the dashed line mark the result for the standard ΛCDM cosmology. We compare with the JWST measurements by Weibel et al. (2024) with the estimate by Akins et al. (2024) (shaded area) who considered the additional contribution by LRD under the assumption that their emission is entirely contributed by stars.

5. Discussion and conclusions

Motivated by recent observational indications for a dynamical behavior of the dark energy, we have explored the possible impact of assuming dynamical DE models with negative cosmological constant on the growth of massive BHs at high redshifts and on the abundance of AGN. We have shown that such cosmological models can account for the observed presence of massive Black Holes with masses $M_{BH} \gtrsim 10^7\, M_\odot$ observed at $z \gtrsim 8$ and for the large over-abundance of AGN at $z \gtrsim 6$ with respect to pre-JWST, without the need to invoke super-Eddington accretion or massive BH seeds. As shown in previous results, the same negative cosmological constant (NCC) models can also account for the large abundance of bright galaxies observed by JWST at $z \gtrsim 10$ and the abundance of massive galaxies at $z \gtrsim 6$, both largely exceeding the pre-JWST expectation in a ΛCDM Universe.

We stress that each of the above observations can in principle be explained by a variety of different astrophysical processes that should become dominant at high redshifts, as discussed in the Introduction. Nevertheless, recent results from different cosmological probes suggest that a departure from ΛCDM toward Dark Energy models may be necessary. Indeed, the indications for an emerging crack in the cosmological constant paradigm are increasing as new analyses of the DESI results (in combination with other cosmological probes) are performed with a variety of different techniques: e.g. in Chaudhary et al. (2026) several DE scenarios are explored, along with cosmologies allowing for spatial curvature, using Metropolis-Hastings Markov Chain Monte Carlo techniques, finding strong statistical evidence for dynamical DE behavior; such a conclusion has been confirmed by analyses extended to consider a wider range of cosmological datasets including DESI DR2 BAO and Lyα data, CMB compressed likelihoods, Big Bang Nucleosynthesis, cosmic chronometers, and multiple Type Ia supernova by Capozziello et al. (2026), and by analyses adopting model-independent techniques to compare the DESI DR1 and DR2 predictions for the ΛCDM model and dynamical DE model for different redshift ranges (Chaudhary et al. 2025). The mounting indications of a departure from ΛCDM calls for the investigations of the impact of the emerging new cosmological scenarios on the interpretations of the JWST observations independently of the possible astrophysical interpretations. Indeed, as showed here, such a new cosmological framework could already by itself account for the enhanced abundances of galaxies and AGN detected at high redshifts observed by JWST. Even if future observations would confirm a downward rescaling of the currently high AGN abundances or BH masses, such as in the "Black Hole Envelope" interpretation (e.g., Umeda et al. 2025, and references therein), NCC cosmologies would still represent a viable background framework to facilitate structure formation without invoking extreme values of the star formation efficiencies or too large initial BH seeds and/or too prolonged super-Eddington accretion phases. More specifically, we found that NCC models with non-phantom behavior, consistent with the results of cosmological probes can account for the JWST observations concerning the properties of the BH, AGN, and galaxy populations at high redshifts. We stress that the region of parameter space that we focused on (see Sect. 3.3) has been selected on the basis of consistency with cosmological probes only, i.e., without considering possible constraints from the observed cosmic reionization history. Although a recent work (Chakraborty et al. 2025) has pointed out that the region of the parameter space we have investigated can be significantly restricted when such constraints are included, such result was obtained under the assumption that reionization is entirely driven by galactic emission; the assumed escape fraction adopted in such work is based on the same assumption. Here, however, we have shown that in NCC scenarios a relevant population of AGN is present at high redshift, with a duty cycle much larger than that of the local Universe, potentially contributing to the reionization, and thus relaxing the constraints on the parameter space. We plan to explore in detail the impact of the assumed cosmological scenario on the cosmic reionization history in a subsequent paper, taking into account the contribution of both galaxies and AGN, with the inclusion of a realistic model to relate the escape fraction in AGN with their feedback on the intergalactic gas.

From a theoretical point of view, our results show a NCC Dark Energy models with a non-phantom equation of state constitute an attractive possibility: in fact, such models:
(i) are naturally motivated in the context of string theory
(ii) allow for consistency with latest CMB+BAO+Sn observations without invoking non-phantom behaviour for the dark energy
(iii) yield finite life time for the Universe with recollapse happening in the future as shown in Mukherjee et al. (2025).

Given that such a theoretically motivated and observationally consistent model can indeed explain the growth of massive BHs and abundances of AGN at high redshift as confirmed by recent JWST measurements, makes such a model highly attractive to pursue as a viable cosmological set up.

Acknowledgements. INAF Theory Grant "AGN-driven outflows in cosmological models of galaxy formation", INAF Mini-grant "Reionization and Fundamental Cosmology with High-Redshift Galaxies", and INAF GO Grant "Revealing the nature of bright galaxies at cosmic dawn with deep JWST spectroscopy". PM acknowledges funding from the Anusandhan National Research Foundation (ANRF), Govt of India, under the National Post-Doctoral Fellowship (File no. PDF/2023/001986). AAS acknowledges the funding from ANRF, Govt of India, under the research grant no. CRG/2023/003984. PM and AAS acknowledge the use of the HPC facility, Pegasus, at IUCAA, Pune, India.

References

Abbott, D. C. T. M. C., Acevedo, M., Aguena, M., et al. 2024, ApJ, 973, L14
Abdul Karim, M., Aguilar, J., Ahlen, S., et al. 2025, Phys. Rev. D, 112, 083515
Abel, T., Bryan, G. L., & Norman, M. L. 2002, Science, 295, 93
Adame, A., Aguilar, J., Ahlen, S., et al. 2025, Journal of Cosmology and Astroparticle Physics, 2025, 021
Adams, N. J., Conselice, C. J., Austin, D., et al. 2024, ApJ, 965, 169
Adil, S. A., Akarsu, O., Di Valentino, E., et al. 2024, Phys. Rev. D, 109, 023527
Adil, S. A., Mukhopadhyay, U., Sen, A. A., & Vagnozzi, S. 2023, JCAP, 10, 072
Aghanim, N. et al. 2020, Astron. Astrophys., 641, A6, [Erratum: Astron.Astrophys. 652, C4 (2021)]
Akins, H. B., Casey, C. M., Lambrides, E., et al. 2024, arXiv e-prints, arXiv:2406.10341
Ananna, T. T., Bogdán, A., Kovács, O. E., Natarajan, P., & Hickox, R. C. 2024, ApJ, 969, L18
Andrade, U., Paillas, E., Mena-Fernández, J., et al. 2025, Validation of the DESI DR2 Measurements of Baryon Acoustic Oscillations from Galaxies and Quasars
Atek, H., Shuntov, M., Furtak, L. J., et al. 2022, MNRAS, 519, 1201–1220
Baggen, J. F. W., van Dokkum, P., Brammer, G., et al. 2024, ApJ, 977, L13
Barausse, E. 2012, MNRAS, 423, 2533
Barlow-Hall, C. L. & Aird, J. 2025, arXiv e-prints, arXiv:2506.16145
Barlow-Hall, C. L., Delaney, J., Aird, J., et al. 2023, MNRAS, 519, 6055
Begelman, M. C., Volonteri, M., & Rees, M. J. 2006, MNRAS, 370, 289–298
Behroozi, P., Conroy, C., Wechsler, R. H., et al. 2020, MNRAS, 499, 5702
Behroozi, P., Wechsler, R. H., Hearin, A. P., & Conroy, C. 2019, MNRAS, 488, 3143
Behroozi, P. S. & Silk, J. 2015, ApJ, 799, 32
Bhowmick, A. K., Blecha, L., Ni, Y., et al. 2022, MNRAS, 516, 138
Bogdán, Á., Goulding, A. D., Natarajan, P., et al. 2024, Nature Astronomy, 8, 126
Bouwens, R., Illingworth, G., Oesch, P., et al. 2023, MNRAS, 523, 1009
Bouwens, R. J., Illingworth, G. D., van Dokkum, P. G., et al. 2022, ApJ, 927, 81
Bromm, V. & Loeb, A. 2003, ApJ, 596, 34–46
Brout, D., Scolnic, D., Popovic, B., et al. 2022, ApJ, 938, 110
Calderón, R., Gannouji, R., L'Huillier, B., & Polarski, D. 2021, Phys. Rev. D, 103, 023526
Calderon, R., Lodha, K., Shafieloo, A., et al. 2024, Journal of Cosmology and Astroparticle Physics, 2024, 048
Caldwell, R. R., Dave, R., & Steinhardt, P. J. 1998, Phys. Rev. Lett., 80, 1582
Cammelli, V., Monaco, P., Tan, J. C., et al. 2024, MNRAS, 536, 851
Capozziello, S., Chaudhary, H., Harko, T., & Mustafa, G. 2026, Physics of the Dark Universe, 51, 102196
Cardenas, R., Gonzalez, T., Leiva, Y., Martin, O., & Quiros, I. 2003, Phys. Rev. D, 67, 083501
Carr, B. J. & Rees, M. J. 1984, MNRAS, 206, 801
Carroll, S. M., De Felice, A., & Trodden, M. 2005, Phys. Rev. D, 71, 023525
Casey, C. M., Akins, H. B., Shuntov, M., et al. 2024, ApJ, 965, 98
Castellano, M., Fontana, A., Treu, T., et al. 2022, ApJ, 938, L15
Chakraborty, A., Choudhury, T. R., Sen, A. A., & Mukherjee, P. 2025, arXiv e-prints, arXiv:2509.02431
Chaudhary, H., Capozziello, S., Praharaj, S., Pacif, S. K. J., & Mustafa, G. 2026, Journal of High Energy Astrophysics, 50, 100507
Chaudhary, H., Capozziello, S., Sharma, V. K., & Mustafa, G. 2025, ApJ, 992, 194
Chevallier, M. & Polarski, D. 2001, Int. J. Mod. Phys. D, 10, 213
Correa, C. A., Wyithe, J. S. B., Schaye, J., & Duffy, A. R. 2015, MNRAS, 450, 1514
Danielsson, U. H. & Van Riet, T. 2018, Int. J. Mod. Phys. D, 27, 1830007
Dayal, P. 2024, A&A, 690, A182
Dayal, P. & Maiolino, R. 2025, arXiv e-prints, arXiv:2506.08116
Dayal, P., Rossi, E. M., Shiralilou, B., et al. 2019, MNRAS, 486, 2336
Dekel, A., Sarkar, K. C., Birnboim, Y., Mandelker, N., & Li, Z. 2023, MNRAS, 523, 3201–3218
Demirtas, M., Kim, M., McAllister, L., Moritz, J., & Rios-Tascon, A. 2021, JHEP, 12, 136
Demirtas, M., Kim, M., McAllister, L., Moritz, J., & Rios-Tascon, A. 2022, Phys. Rev. Lett., 128, 011602
Di Valentino, E., Mukherjee, A., & Sen, A. A. 2021, Entropy, 23, 404
Dodelson, S. 2003, Modern Cosmology (Academic Press, Elsevier Science)
Donnan, C. T., McLeod, D. J., Dunlop, J. S., et al. 2022, MNRAS, 518, 6011
Donnan, C. T., McLeod, D. J., McLure, R. J., et al. 2023, MNRAS, 520, 4554
Dutta, K., Ruchika, Roy, A., Sen, A. A., & Sheikh-Jabbari, M. M. 2020, Gen. Rel. Grav., 52, 15
Fan, X., Bañados, E., & Simcoe, R. A. 2023, ARA&A, 61, 373
Ferrara, A. 2024, A&A, 684, A207
Finkelstein, S. L., Bagley, M. B., Arrabal Haro, P., et al. 2022, ApJ, 940, L55
Finkelstein, S. L., Bagley, M. B., Ferguson, H. C., et al. 2023, apjl, 946, L13
Finkelstein, S. L., Leung, G. C. K., Bagley, M. B., et al. 2024, ApJL, 969, L2
Furtak, L. J., Labbé, I., Zitrin, A., et al. 2024, Nat, 628, 57
Furtak, L. J., Zitrin, A., Plat, A., et al. 2023, ApJ, 952, 142
Gelli, V., Mason, C., & Hayward, C. C. 2024, ApJ, 975, 192
Giallongo, E., Grazian, A., Fiore, F., et al. 2015, A&A, 578, A83
Giallongo, E., Grazian, A., Fiore, F., et al. 2019, ApJ, 884, 19
Giarè, W., Najafi, M., Pan, S., Di Valentino, E., & Firouzjaee, J. T. 2024, Journal of Cosmology and Astroparticle Physics, 2024, 035
Glikman, E., Djorgovski, S. G., Stern, D., et al. 2011, ApJ, 728, L26
Graña, M. & Herráez, A. 2021, Universe, 7, 273
Grazian, A., Boutsia, K., Giallongo, E., et al. 2023, ApJ, 955, 60
Greene, J. E., Labbe, I., Goulding, A. D., et al. 2024, ApJ, 964, 39
Harikane, Y., Ouchi, M., Oguri, M., et al. 2023, ApJSupplement Series, 265, 5
Harikane, Y., Zhang, Y., Nakajima, K., et al. 2023a, ApJ, 959, 39
Harikane, Y., Zhang, Y., Nakajima, K., et al. 2023b, ApJ, 959, 39
Inayoshi, K. & Ichikawa, K. 2024, Birth of Rapidly Spinning, Overmassive Black Holes in the Early Universe
Juodžbalis, I., Maiolino, R., Baker, W. M., et al. 2025, arXiv e-prints, arXiv:2504.03551
Juodžbalis, I., Maiolino, R., Baker, W. M., et al. 2024, Nature, 636, 594–597
Kocevski, D. D., Finkelstein, S. L., Barro, G., et al. 2025, ApJ, 986, 126
Kocevski, D. D., Onoue, M., Inayoshi, K., et al. 2023, ApJ, 954, L4
Kokorev, V., Caputi, K. I., Greene, J. E., et al. 2024, ApJ, 968, 38
Kokorev, V., Fujimoto, S., Labbe, I., et al. 2023, ApJL, 957, L7
Kovács, O. E., Bogdán, Á., Natarajan, P., et al. 2024, ApJ, 965, L21
Labbe, I., Greene, J. E., Bezanson, R., et al. 2025, ApJ, 978, 92
Labbé, I., van Dokkum, P., Nelson, E., et al. 2023, Nat, 616, 266–269
Lacey, C. & Cole, S. 1993, MNRAS, 262, 627
LaChance, P., Croft, R. A. C., Di Matteo, T., et al. 2025, arXiv e-prints, arXiv:2505.20439
Lai, S., Onken, C. A., Wolf, C., Bian, F., & Fan, X. 2024, MNRAS, 531, 2245
Latif, M. A., Whalen, D. J., Khochfar, S., Herrington, N. P., & Woods, T. E. 2022, Nat, 607, 48–51
Linder, E. V. 2003, Phys. Rev. Lett., 90, 091301
Linder, E. V. 2006, Phys. Rev. D, 73, 063010
Linder, E. V. 2008a, Rept. Prog. Phys., 71, 056901
Linder, E. V. 2008b, Gen. Rel. Grav., 40, 329
Liu, Y., Gao, L., Bose, S., et al. 2024, MNRAS, 527, 11740
Lodha, K., Calderon, R., Matthewson, W. L., et al. 2025, Phys. Rev. D, 112, 083511
Lodha, K., Shafieloo, A., Calderon, R., et al. 2025, Phys. Rev. D, 111, 023532
Louis, T. et al. 2025, JCAP, 11, 062
Ludwick, K. J. 2017, Modern Physics Letters A, 32, 1730025
Lupi, A., Quadri, G., Volonteri, M., Colpi, M., & Regan, J. A. 2024, A&A, 686, A256
Luu, H. N., Qiu, Y.-C., & Tye, S.-H. H. 2025, Phys. Rev. D, 112, 023524
Madau, P., Haardt, F., & Dotti, M. 2014, ApJ, 784, L38
Madau, P. & Rees, M. J. 2001, ApJ, 551, L27
Maiolino, R., Scholtz, J., Curtis-Lake, E., et al. 2024a, A&A, 691, A145
Maiolino, R., Scholtz, J., Witstok, J., et al. 2024b, Nat, 627, 59
Maiolino, Roberto, Scholtz, Jan, Curtis-Lake, Emma, et al. 2024, A&A, 691, A145
Maldacena, J. M. 1998, Adv. Theor. Math. Phys., 2, 231
Malekjani, M., Conville, R. M., Colgáin, E. O., Pourojaghi, S., & Sheikh-Jabbari, M. M. 2024, Eur. Phys. J. C, 84, 317
Mason, C. A., Trenti, M., & Treu, T. 2015, ApJ, 813, 21
Matthee, J., Naidu, R. P., Brammer, G., et al. 2024, ApJ, 963, 129
McClymont, W., Tacchella, S., Ji, X., et al. 2026, MNRAS, 545, staf2092
McLeod, D. J., Donnan, C. T., McLure, R. J., et al. 2023, MNRAS, 527, 5004
Menci, N., Adil, S. A., Mukhopadhyay, U., Sen, A. A., & Vagnozzi, S. 2024a, JCAP, 2024, 072
Menci, N., Castellano, M., Santini, P., et al. 2022, ApJ, 938, L5
Menci, N., Sen, A. A., & Castellano, M. 2024b, ApJ, 976, 227
Mukherjee, P., Kumar, D., & Sen, A. A. 2025, arXiv e-prints, arXiv:2501.18335
Murai, K. & Takahashi, F. 2025, Phys. Rev. D, 112, 103501
Neistein, E., Van Den Bosch, F. C., & Dekel, A. 2006, MNRAS, 372, 933

Ni, Y., Di Matteo, T., Bird, S., et al. 2022, MNRAS, 513, 670
Nojiri, S., Odintsov, S. D., & Tsujikawa, S. 2005, Phys. Rev. D, 71, 063004
Oikonomou, V. K. & Giannakoudi, I. 2022, Int. J. Mod. Phys. D, 31, 2250075
Padmanabhan, T. 2002, Theoretical Astrophysics - Volume 3, Galaxies and Cosmology, Vol. 3 (Cambridge: Cambridge Univ. Press)
Palti, E. 2019, Fortsch. Phys., 67, 1900037
Peacock, J. A. 1999, Cosmological Physics (Cambridge: Cambridge Univ. Press)
Peebles, P. J. E. & Ratra, B. 1988, ApJ, 325, L17
Perkovic, D. & Stefancic, H. 2020, Eur. Phys. J. C, 80, 629
Perlmutter, S. et al. 1999, ApJ, 517, 565
Porras-Valverde, A. J., Ricarte, A., Natarajan, P., et al. 2025, arXiv e-prints, arXiv:2504.11566
Poulin, V., Boddy, K. K., Bird, S., & Kamionkowski, M. 2018, Phys. Rev. D, 97, 123504
Pérez-González, P. G., Costantin, L., Langeroodi, D., et al. 2023, ApJ, 951, L1
Pérez-González, P. G., Östlin, G., Costantin, L., et al. 2025, The rise of the galactic empire: luminosity functions at $z \sim 17$ and $z \sim 25$ estimated with the MIDIS+NGDEEP ultra-deep JWST/NIRCam dataset
Quadri, G., Trinca, A., Lupi, A., Colpi, M., & Volonteri, M. 2025, arXiv e-prints, arXiv:2505.05556
Ratra, B. & Peebles, P. J. E. 1988, Phys. Rev. D, 37, 3406
Riess, A. G., Filippenko, A. V., Challis, P., et al. 1998, AJ, 116, 1009
Robertson, B., Johnson, B. D., Tacchella, S., et al. 2024, ApJ, 970, 31
Rubin, D., Aldering, G., Betoule, M., et al. 2025, Union Through UNITY: Cosmology with 2,000 SNe Using a Unified Bayesian Framework
Ruchika, Adil, S. A., Dutta, K., Mukherjee, A., & Sen, A. A. 2023, Phys. Dark Univ., 40, 101199
Sánchez, B. O. et al. 2024, ApJ, 975, 5
Schauer, A. T. P., Regan, J., Glover, S. C. O., & Klessen, R. S. 2017, MNRAS, 471, 4878
Scherrer, R. J. 2015, Phys. Rev. D, 92, 043001
Scholtz, J., Maiolino, R., D'Eugenio, F., et al. 2025, A&A, 697, A175
Scolnic, D., Brout, D., Carr, A., et al. 2022, ApJ, 938, 113
Sen, A. A., Adil, S. A., & Sen, S. 2022, Mon. Not. Roy. Astron. Soc., 518, 1098
Shen, X., Hopkins, P. F., Faucher-Giguère, C.-A., et al. 2020, MNRAS, 495, 3252
Shen, X., Vogelsberger, M., Boylan-Kolchin, M., Tacchella, S., & Kannan, R. 2023, MNRAS, 525, 3254
Sheth, R. K. & Tormen, G. 1999, MNRAS, 308, 119
Somerville, R. S., Yung, L. Y. A., Lancaster, L., et al. 2025, MNRAS
Sun, G., Faucher-Giguère, C.-A., Hayward, C. C., et al. 2023, ApJ, 955, L35
Svrcek, P. 2006, arXiv e-prints, hep-th/0607086, hep
Sánchez, B. O., Brout, D., Vincenzi, M., et al. 2024, ApJ, 975, 5
Taylor, A. J., Finkelstein, S. L., Kocevski, D. D., et al. 2024, arXiv e-prints, arXiv:2409.06772
Trinca, A., Schneider, R., Valiante, R., et al. 2024a, MNRAS, 529, 3563
Trinca, A., Valiante, R., Schneider, R., et al. 2024b, arXiv e-prints, arXiv:2412.14248
Trivedi, O. 2024, Symmetry, 16, 298
Umeda, Hiroya andx Inayoshi, K., Harikane, Y., & Murase, K. 2025, arXiv e-prints, arXiv:2512.04208
Vafa, C. 2005, arXiv e-prints, hep-th/0509212, hep
Vikman, A. 2005, Phys. Rev. D, 71, 023515
Vincenzi, M., Brout, D., Armstrong, P., et al. 2024, ApJ, 975, 86
Visinelli, L., Vagnozzi, S., & Danielsson, U. 2019, Symmetry, 11, 1035
Volonteri, M., Haardt, F., & Madau, P. 2003, ApJ, 582, 559
Volonteri, M., Habouzit, M., & Colpi, M. 2021, Nature Reviews Physics, 3, 732
Volonteri, M., Silk, J., & Dubus, G. 2015, ApJ, 804, 148
Volonteri, M., Trebitsch, M., Dubois, Y., et al. 2024, arXiv e-prints, arXiv:2408.12854
Wang, H., Peng, Z.-Y., & Piao, Y.-S. 2025, Phys. Rev. D, 111, L061306
Wechsler, R. H., Bullock, J. S., Primack, J. R., Kravtsov, A. V., & Dekel, A. 2002, ApJ, 568, 52
Weibel, A., Oesch, P. A., Barrufet, L., et al. 2024, MNRAS, 533, 1808
Wetterich, C. 1995, Astron. Astrophys., 301, 321
Whitler, L., Endsley, R., Stark, D. P., et al. 2022, MNRAS, 519, 157
Xiao, M., Oesch, P., Elbaz, D., et al. 2024, Accelerated Formation of Ultra-Massive Galaxies in the First Billion Years
Yung, L. Y. A., Somerville, R. S., Finkelstein, S. L., Wilkins, S. M., & Gardner, J. P. 2023, MNRAS, 527, 5929
Zhu, Q., Li, Y., Li, Y., et al. 2022, MNRAS, 514, 5583